Complementary polytopic interactions (CPI) as revealed by molecular modelling using the XED force field

Owen R. Lozman,* Richard J. Bushby and Jeremy G. Vinter†

SOMS Centre, University of Leeds, Woodhouse Lane, Leeds, West Yorkshire, UK LS4 2NQ.
E-mail: owenl@chem.leeds.ac.uk; Fax: 44 (0)113 233 6452; Tel: 44 (0)113 233 4992

Received (in Cambridge, UK) 17th April 2001, Accepted 22nd June 2001
First published as an Advance Article on the web 9th August 2001

To explain 1 : 1 compound formation between HAT (2,3,6,7,10,11-hexaalkoxytriphenylene) discogens and PTP (2,3,6,7,10,11-hexakis(4-alkylphenyl)triphenylene or PDQ (2,3,6,7,10,11-hexakis(4-alkylphenyl)dipyrazino-[2,3,-*f*:2′,3′-*h*]quinoxaline) derivatives we have exploited the XED (extended electron distribution) force field method. This is the only method that we have found which is able to explain why compound formation occurs in some cases but not in others. Not only is the force field successful in the case of these discogens and in a number of systems investigated by Hunter and Rebek, but we also show that it can explain the observed stability of other π-stacked systems including HAT–TNF (trinitrofluorenone), benzene–hexafluorobenzene, triphenylene–perfluorotriphenylene, benzene multiyne–TNF systems and complementary mixtures of selectively fluorinated 1,4-bis(phenylethynyl)benzene derivatives. In each case the interaction is expressed as a sum of atom-based van der Waals and multipole interactions: a complementary polytopic interaction.

Introduction

Single electron transfer has been a major theme of the research of Professor Eberson and indeed of physical organic chemistry over the last fifty years.[1] Charge-transfer interactions have often been invoked to explain the stability of $(AB)_n$ π-stacked systems. However, this idea has recently been challenged and it has been argued that, even when alternating two component π-stacked systems show a charge-transfer interaction, this is not the major source of their stability.

Indeed, during our investigations into discotic liquid crystals we discovered a very stable $(AB)_n$ system (**1a**–**2a**, Fig. 1) in which there is no detectable charge-transfer band.[2–4] In this case it is clear that charge transfer is not the source of the stabilising π-stacking interaction. Neither can it be ascribed to matched net quadrupolar interactions between the two components. Rather, we have shown that the structure and stability of **1a**–**2a** can be explained using an XED (extended electron distribution) force field. This same approach is also shown to apply to many related systems.

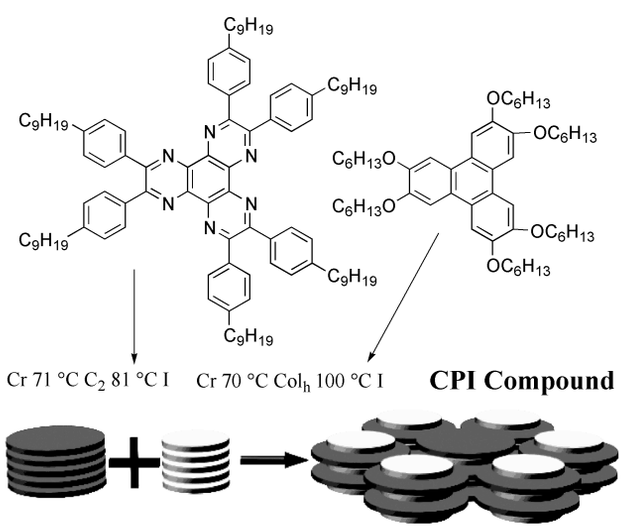

Fig. 1 Schematic representation of the packing of **1** and **2** into a hexagonal columnar arrangement with alternating AB stacks.[2]

Charge-transfer interactions arise out of the coupling between the molecular orbitals of adjacent molecules. This perturbation of the wave functions gives rise to distinct bands in the UV absorption spectrum of the mixture that are not present in the component spectra. For example, in mixtures of **1a** with 2,4,7-trinitrofluoren-9-one (TNF, **3**, Scheme 1), a good electron acceptor, there is a colour change as a result of the charge-transfer interaction. Despite this it seems unlikely that this charge transfer explains the stability of the **1a**–**3** mixture. The work of Bates and Luckhurst shed new light on this particular case.[5] They used molecular dynamics simulations to show that the phase behaviour of the mixtures could be reproduced by Gay–Berne particles bearing net quadrupoles that were opposite in sign. However, in the case of mixtures of **1a**–**2a** there is no colour change and no new absorption bands are present in the UV/VIS spectrum.[2] Unlike the mixtures studied by Bates and Luckhurst, the "net quadrupole" explanation also fails (Table 1). Rather, we found, as Hunter and Sanders did from their study of intermolecular interactions in porphyrins, that: "*It is the properties of the atoms at the points of intermolecular contact rather than the overall redox properties of the molecules, which determine how π-systems interact*."[6]

In order to explore the subtleties of the interaction at the points of individual molecular contact we looked at several approaches. For small molecules, the most reliable *ab initio* and semi-empirical methods can be employed but for larger molecules these methods become unwieldy and bear a high computational burden. In order to surmount this problem a force field method was chosen greatly reducing the computational burden. Following on from the work of Hunter and Sanders, a force field was developed that more accurately describes the charge distribution of the molecules.

In the XED (extended electron distribution) force field, an initial single point calculation is used to calculate the charge distribution across atomic centres (Fig. 2, left). The nuclear charge of atoms with π-bonds or lone pairs is then incremented

† J.G.V. can be contacted by e-mail: jgv10@cam.ac.uk.

 DOI: 10.1039/b103390p

Table 1 Summary of the quadrupole moments for a selection of the molecules encountered in this paper. The quadrupole moments were calculated at the PM3 level on the minimum energy conformation produced by the XED conformational search engine

Molecule	Quadrupole moment/e Å^2	Compound formed	Compound predicted
Benzene (C_6H_6)	−16.7	Yes	Yes
C_6F_6	17.8		
Triphenylene (tp)	3.9	Yes	No
12F-tp	14.6		
HAT1 (**1b**)	−24.6		
TNF (**3**)	67.1	Yes[a]	Yes[b]
PDQ1 (**2e**)	43.1	Yes[a]	Yes[b]
PTP1 (**2f**)	−71.2	Yes[a]	No[b]
PTPO1 (**2g**)	29.4	Yes[a]	Yes[b]
PDQ2O1 (**2h**)	0.2	No[a]	Yes[b]
PTP2O1 (**2i**)	−39.0	No[a]	No[b]
XPTP2O1 (**4b**)	−45.6	No[a]	No[b]

[a] Compound formation observed experimentally when the long chain analogue is mixed with HAT6 (**1a**). [b] Stable mixture predicted on the basis of the interaction between net quadrupoles of the molecules with HAT1 (**1b**).

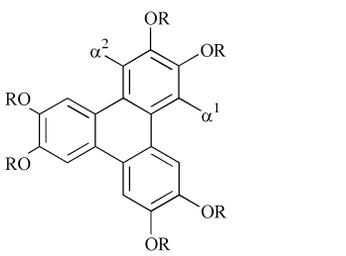

1a HAT6 $\alpha^1=\alpha^2$=H, R=OC_6H_{13}
1b HAT1 $\alpha^1=\alpha^2$=H, R=OCH_3
1c NO_2-HAT6 $\alpha^1=NO_2$, α^2=H, R=OC_6H_{13}
1d NO_2-HAT1 $\alpha^1=NO_2$, α^2=H, R=OCH_3
1e 2F-HAT6 $\alpha^1=\alpha^2$=F, R=OC_6H_{13}
1f 2F-HAT1 $\alpha^1=\alpha^2$=F, R=OCH_3
1n HATn α^1=H, R=C_nH_{2n+1}

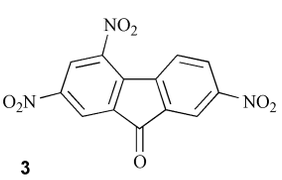

3

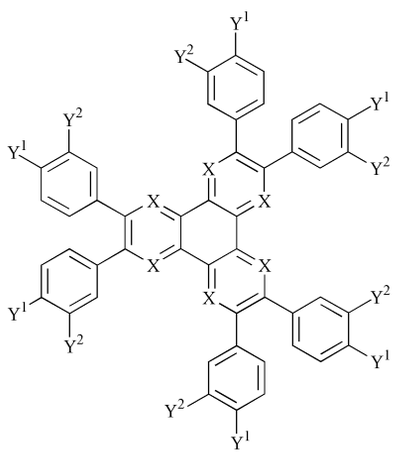

2a PDQ9 X=N, $Y^1=C_9H_{19}$, Y^2=H
2b PTP9 X=CH, $Y^1=C_9H_{19}$, Y^2=H
2c PDQ2O6 X=N, $Y^1=Y^2=OC_6H_{13}$
2d PDP2O6 X=CH, $Y^1=Y^2=OC_6H_{13}$
2e PDQ1 X=N, $Y^1=CH_3$, Y^2=H
2f PTP1 X=CH, $Y^1=CH_3$, Y^2=H
2g PTPO1 X=CH, $Y^1=OCH_3$, Y^2=H
2h PDQ2O1 X=N, $Y^1=Y^2=OCH_3$
2i PTP2O1 X=CH, $Y^1=Y^2=OCH_3$

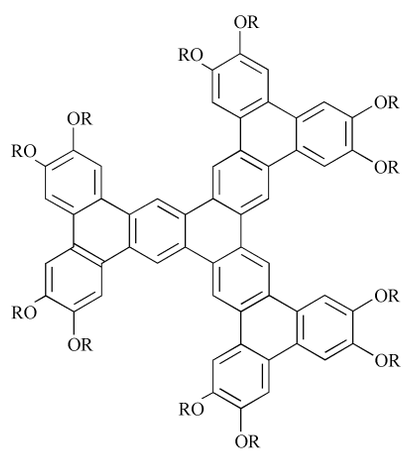

4a xPTP2O6 R=C_6H_{13}
4b xPTP2O1 R=CH_3

Scheme 1 Molecules used in the investigation of CPI interactions and the short chain analogues used in the XED modelling.

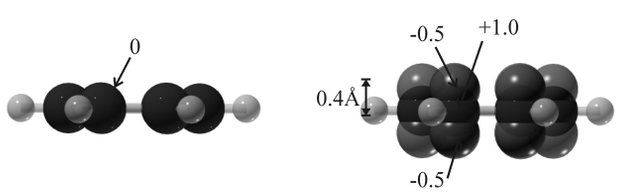

Fig. 2 Comparison of ACC and XED descriptions of benzene.

and the electrons are placed at a pre-defined distance from the atomic centres (Fig. 2, right).[7]

In this paper we show how the XED force field can be used to successfully predict mixture formation between **1a** and **2a**, related systems and previously published data for alkoxytriphenylenes and benzene multiynes mixed with TNF[8] and selectively fluorinated 1,4-bis(phenylethynyl)benzenes.[9]

Experimental

The geometries of the molecules under investigation were optimised using the AM1 semi-empirical routine in MOPAC.[7,10] After the extended electrons were added a conformational search was performed using the XED force field.[7]

The general form of the force field [eqn. (1)] is based on the

$$E = E_b + E_a + E_t + E_{VDW} + E_{coul} \quad (1)$$

usual molecular mechanics principles in which the total energy (E) is comprised of the sum of bond stretch (E_b), bond angle deformation (E_a), a periodic torsional barrier (E_t), van der Waals (E_{VDW}) and coulombic terms (E_{coul}).[11]

The global minima from the conformational analysis were then docked in pairs using a free SIMPLEX minimiser.[10] This involves holding one of the molecules stationary whilst another molecule (bullet) is moved along a "valley" on the potential energy surface (Fig. 3). This process is then repeated for a total of 250 bullets with different starting positions, which are distributed evenly around the surface of a sphere. Full details of the routines and the XED force-field parametrisation are given in ref. 7.

The output from the docking experiment gives the overall interaction energy and its VDWs and coulombic contributions. By comparing the interactions between the molecules and

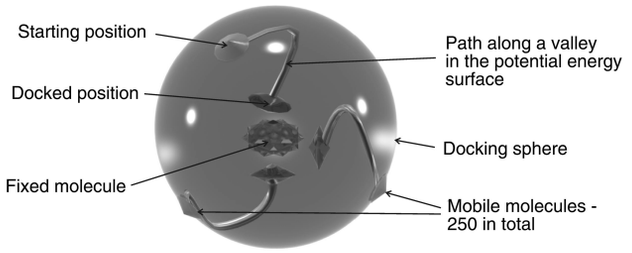

Fig. 3 Schematic illustration of the docking procedure. In the docking of two molecules, one is fixed at the centre of a sphere; the mobile molecule is moved from a total of 250 different starting positions.

themselves (*i.e.* U_{AA} and U_{BB}) with the mixed system (*i.e.* U_{AB}) it is possible to predict whether or not a stable mixture should be formed. The results are used to quantify this difference in interaction with the term ΔE, defined in eqn. (2).

$$\Delta E = U_{AB} - \tfrac{1}{2}(U_{AA} + U_{BB}) \quad (2)$$

A compound is predicted to form if ΔE carries a negative value.

Results and discussion

Table 1 shows calculated values for the net quadrupoles of a selection of aromatic cores and the predicted stability or otherwise of mixtures based on the net quadrupolar model. It is evident from these results that the interaction of net quadrupoles does not always account for the experimentally observed stabilisation.

Compounds **2a** and **2b** have different electronic characteristics but similar shapes and comparable space-filling characteristics. Mixtures of both **2a** and **2b** with HAT discogens of varying chain lengths **1*n*** (n = 4–16) behave in much the same way.[2] In both cases there is an optimum side-chain length for the **1*n*** component, presumably corresponding to the same optimum packing (see Fig. 5, ref. 2). The stabilising CPI effect disappears in those systems where there is greater steric congestion in close proximity to the aromatic core and no stable mixtures are obtained for the systems **1a**–**2c** or **1a**–**2d** in which the number of side-chains is doubled to twelve.[4] The complementary packing of the side-chains is therefore important but it fails to explain the differences between the quinoxaline (**1a**–**2a**) and triphenylene (**1a**–**2b**) based systems. Nor is there any evidence from density measurements that there is an unusually small free volume or unusually favourable packing in these mixtures.‡ For these reasons we have opted to simplify the molecular modelling by restricting the chain lengths of the compounds. In the following section we illustrate the ways in which XED can explain the stability of some of these systems where the simple net quadrupolar explanation often fails.

Benzene (mp 5.5 °C) and hexafluorobenzene (mp 4 °C) form a stable 1 : 1 compound, the melting point of which is higher than that of either of the components (mp 24 °C).[12] The same situation occurs in mixtures of triphenylene (mp 199 °C) with its perfluorinated analogue (mp 109 °C), where a marked temperature increase is observed (mp 250–252 °C).[13] These systems are therefore ideal candidates to test the XED force field and compare the difference between ACC (atom centred charge)[14] and XED (extended electron distribution) calculations for small and medium sized molecules.

‡ Densities were estimated from X-ray diffraction measurements of the unit cell parameters (at T °C): **1a** (95 °C) = 0.67 g cm^{-3}, **2a** (50 °C) = 0.73 g cm^{-3}, **2b** (50 °C) = 0.77 g cm^{-3}, **1a**–**2a** (100 °C) = 0.68 g cm^{-3}, **1a**–**2b** (100 °C) = 0.73 g cm^{-3}.

Comparison of XED and ACC methods for benzene and hexafluorobenzene.

In the case of benzene–hexafluorobenzene both methods agree that the hetero-dimer is more stable than either of the homo-dimers (Table 2). However, the geometry of the interacting species is in closer agreement with experiment if XEDs are included in the force field.[15] A recent study of the benzene–hexafluorobenzene supramolecular synthon shows that very high levels of theory are needed to predict the experimental observations.[16] These results are compared to the values calculated by the XED force field and the estimations made by Williams from his detailed analysis of the crystal structure in Table 3.[17]

Comparison of XED and ACC methods for triphenylene and perfluorotriphenylene

The geometries of the dimers are closer to those obtained from X-ray diffraction studies when extended electrons are included in the force field.[13] Both methods correctly predict that the hetero-dimer has a lower energy minimum then either of the homo-dimers. In this case the difference in the estimation of the coulombic contribution to the total interaction energy predicted using XED or ACC methods becomes more apparent (Table 4). The predicted intermolecular distance in the 1 : 1 mixture of triphenylene and perfluorotriphenylene is 3.5–3.7 Å, the same as that observed in the single crystal X-ray structure. In summary, the use of a distributed multipole model as invoked by the XED force field, produces significantly better matches to the known geometries for intermolecular aromatic dimers of benzene and triphenylene with their perfluorinated analogues. On moving from small to medium sized molecules inclusion of extended electrons tends to increase the estimation of the coulombic contribution to the overall interaction energy.

XED modelling of the CPI discotic liquid crystals (1–2 or –4): variations in the structure of the large core component

Stability of the mixtures. The results of the docking experiments for HAT1 (**1b**), derivatives of PTP and PDQ (**2**) and their complementary mixtures are shown in Table 5. Those mixtures that form compounds are correctly predicted to have a negative value of ΔE. The VDW and coulombic contributions to ΔE, shown in Table 6, allow a comparison of their relative importance in determining whether or not the mixture will form a stable compound.

In the case where the mixture forms a compound, the hetero-dimer is stabilised by a favourable coulombic contribution. For PDQ1–HAT1 (**2e**–**1b**) the VDW contribution is repulsive and the hetero-dimer is stabilised solely by the coulombic attraction, which is greater than that between the molecules in the corresponding homo-dimers. The hetero-dimer containing either PTP1 (**2f**) or PTPO1 (**2g**), is further stabilised by a favourable VDW attraction.

For the mixtures comprising the more highly substituted molecules PDQ2O1 (**2h**) or PTP2O1 (**2i**) the situation is reversed and the homo-dimers are predicted to be more stable than the hetero-dimer with HAT1 (**1b**). The hetero-dimer PDQ2O1–HAT1 (**2h**–**1b**) is destabilised by an unfavourable coulombic contribution, probably due to the extra electron density around the aromatic core in comparison to PDQ1 (**2e**). PTP2O1 (**2i**)–HAT1 (**1b**) does not form a stable compound because in the PTP2O1 (**2i**) homo-dimer the molecules have a higher surface contact area resulting in a much more favourable VDW contribution.

When the peripheral phenyl groups are fused to the core, as is the case with xPTP2O1 (**4b**), the surface area of molecular contact is increased dramatically, as is the degree of conjugation. In the case of the homo-dimer the molecules of xPTP2O1 (**4b**) pack efficiently, producing a favourable VDW and coulombic

Table 2 Comparison of calculated VDWs and coulombic contributions to the energies of homo- and hetero-dimers of benzene (C_6H_6) and hexafluorobenzene (C_6F_6) with (and without) the inclusion of XEDs in the force field

	With XEDs (without XEDs)			
Mixture	E_{VDW}/kcal mol^{-1}	E_{coul}/kcal mol^{-1}	Total energy/kcal mol^{-1}	ΔE/kcal mol^{-1}
$C_6H_6 \times 2$	−3.54 (−5.03)	−1.13 (−0.18)	−4.68 (−5.21)	—
$C_6F_6 \times 2$	−7.42 (−6.91)	1.9 (0.98)	−5.33 (−5.93)	—
$C_6H_6 + C_6F_6$	−7.68 (−7.67)	−2.9 (−2.17)	−10.59 (−9.84)	−5.6 (−4.3)

Table 3 Comparison of the intermolecular distance and energy of interaction in the benzene–hexafluorobenzene supramolecular synthon as calculated by different *ab initio*, semi-empirical and force field methods

Method	Ref.	Separation/Å	ΔE/kcal mol^{-1}
Experiment	17	3.4–3.6	~−7
CP-MP2/6-31G**	16	3.6	−3.7
HF/6-31G**	16	4.1	−1.5
AM1	16	4.7	−0.5
PM3	16	4.5	−0.5
XEDs	—	3.6	−5.6
ACCs	—	3.3	−4.2

contribution in comparison with the xPTP2O1–HAT1 (**4b**–**1b**) hetero-dimer. The longer chain derivatives xPTP2O6 (**4a**) and HAT6 (**1a**) are immiscible.

In summary, it appears that the stable mixtures formed are due to favourable van der Waals and coulombic interactions between the large and small components. In the hexa-substituted large-core molecules, the VDW interactions in the homo-dimers are relatively weak, and the VDW energy of the dimer is lowered if one of the large core components is replaced with HAT1 (**1b**). In each case the hetero-dimer containing the dodeca-substituted molecules is predicted not to form, although different factors contribute in each case.

It is apparent from these results that there is no simple relationship between the molecular structures of the molecules and the dominant factor in determining which of the homo- or hetero-dimers is more stable. In order to successfully predict the formation of π-stacked binary mixtures of aromatic molecules, it is essential that the interactions at each individual point of molecular contact be accounted for. The sum of the relatively low energy interactions between the π-stacked molecules gives rise to a many site (Greek: polytopic) interaction between molecules with complementary shapes and/or electron distributions. Hence we have termed this new macromolecular synthon the "complementary polytopic interaction" or CPI.

Geometries of the dimers. The cores of HAT1 (**1b**) in the homo-dimer are slightly staggered within the stack and there is also a degree of lateral displacement in the plane of the core (Fig. 4, left). These observations compare favourably with the single crystal X-ray diffraction results obtained for a similar triphenylene containing species TP6EO2M [18] and electron diffraction experiments for HAT5.[19] The PDQ1 (**2e**) homo-dimer adopts a staggered conformation and in this case there is a large amount of lateral displacement (Fig. 4, middle). The interactions between the peripheral phenyl groups and between the

Table 5 The minimum energies (and coulombic and VDW contributions) calculated by the XED docking procedure for HAT1 (**1b**), PDQ1 (**2e**), PTP1 (**2f**), PTPO1 (**2g**), PDQ2O1 (**2h**), PTP2O1 (**2i**), xPTP2O1 (**4b**) and their complementary mixtures. All energies are in kcal mol^{-1}

					Mix with **1b**?	
Mixture	E_{VDW}	E_{coul}	Total energy	ΔE	[a]	[b]
1b	−37.4	−2.4	−39.8		—	—
2e	−39.7	0.8	−38.9		—	—
2e–**1b**	−37.7	−4.1	−41.2	−1.9	Y	Y
2f	−45.9	9.7	−36.2		—	—
2f–**1b**	−43.8	−6.2	−49.9	−11.9	Y	Y
2g	−37.2	−7.8	−45.0		—	—
2g–**1b**	−44.1	−6.5	−50.5	−8.1	Y	Y
2h	−38.8	−12.8	−51.6		—	—
2h–**1b**	−37.1	−3.8	−40.9	4.8	N	N
2i	−45.1	2.1	−41.0		—	—
2i–**1b**	−28.0	−4.6	−32.6	7.8	N	N
4b	−83.9	−7.3	−91.2		—	—
4b–**1b**	−34.9	0.4	−34.5	31.0	N	N

[a] Compound formed by a 1 : 1 molar mixture of HAT6 (**1a**) with the long chain analogue of the large molecule. [b] Compound predicted by comparison of the minimum energy of docked homo-dimers with that of the HAT1 (**1b**) containing hetero-dimers.

phenyl group of one molecule and the aza-triphenylene core of another appear to produce the dominant contribution to the CPI. In the HAT1 (**1b**)–PDQ1 (**2e**) hetero-dimer the molecules show only very slight deviation from the fully staggered geometry and there is no lateral displacement in the plane of the aromatic core (Fig. 4, right). The major contribution to the CPI is the attraction between the central cores and the attraction between the peripheral phenyl groups of PDQ1 (**2e**) with the triphenylene core of HAT1 (**1b**).

The minimum energy geometry for the HAT1–PDQ1 (**1b**–**2e**) hetero-dimer was used as a new starting point (as the fixed central "molecule") after its charge distribution was recalculated. HAT1 (**1b**) was observed to dock preferentially with the PDQ1 side of the dimer, whilst PDQ1 (**2e**) docked preferentially with the HAT1 side of the dimer. The alternate "wrong" docks (HAT1 (**1b**) with the HAT1 side for example) were at least 20 kcal mol^{-1} less stable. For comparison the energies of the minimum energy geometries are shown in Table 7. These results show that there is no difference in the enthalpy change associated with the docking of subsequent molecules.

The homo-dimer of PDQ2O1 (**2h**), which has a higher atomic density in proximity to the aromatic core, prefers the quinoxaline cores in more intimate contact than the equivalent

Table 4 Comparison of calculated VDWs and coulombic contributions to the energies of homo- and hetero-dimers of triphenylene (tp) and perfluorotriphenylene (12F-tp) with (and without) the inclusion of XEDs in the force field

	With XEDs (without XEDs)			
Mixture	E_{VDW}/kcal mol^{-1}	E_{coul}/kcal mol^{-1}	Total energy/kcal mol^{-1}	ΔE/kcal mol^{-1}
tp × 2	−25.13 (−25.63)	5.88 (1.83)	−19.24 (−23.80)	—
12F-tp × 2	−26.96 (−25.83)	−2.48 (3.86)	−29.45 (−21.96)	—
Tp + 12F-tp	−23.96 (−24.83)	−9.66 (−4.02)	−33.62 (−24.85)	−9.3 (−1.97)

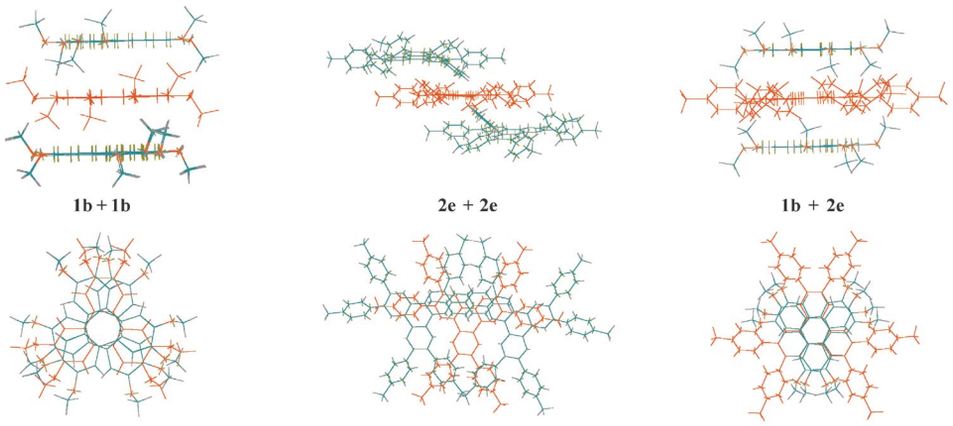

Fig. 4 Predicted minimum energy geometries of π-stacked dimers: left, HAT1 (**1b**) homo-dimer; middle PDQ1 (**2e**) homo-dimer; right HAT1–PDQ1 (**1b**–**2e**) hetero-dimer. The upper section shows the side view and lower shows the plan view. The central (red) molecule is held fixed; the other (blue) molecules are the bullets that dock to the lowest energies. In each case both possible sites (above and below) are shown.

Table 6 Summary of the relative contributions of VDW and coulombic interactions to ΔE for the results shown in Table 5

Mixture with HAT1 (**1b**)	ΔE_{coul}/kcal mol^{-1}	ΔE_{VDW}/kcal mol^{-1}	ΔE_{Total}/kcal mol^{-1}
PDQ1 (**2e**)	−2.9	0.8	−1.9
PTP1 (**2f**)	−9.9	−2.0	−11.9
PTPO1 (**2g**)	−1.4	−6.8	−8.1
PDQ2O1 (**2h**)	5.8	−1.0	4.8
PTP2O1 (**2i**)	−5.1	13.3	7.8
XPTP2O1 (**4b**)	5.3	25.8	31.0

Table 7 The minimum energies (and their coulombic and VDW contributions) (in kcal mol^{-1}) calculated by the XED docking procedure for HAT1 (**1a**) and PDQ1 (**2e**) stacks

Molecule	E_{VDW}	E_{coul}	E_{Total}	ΔE
PDQ1 (**2e**)	−37.4	−2.4	−39.8	
HAT1 (**1b**)	−39.7	0.8	−38.9	
2e–**1b**	−37.7	−4.1	−41.2	−1.9
{**2e**–**1b**}–**1b**	−38.6	−5.52	−43.6	−2.2[a]
{**2e**–**1b**}–**2e**	−39.2	−3.52	−42.8	−1.7[a]

[a] ΔE calculated per interacting ring, with respect to the component homo-dimers.

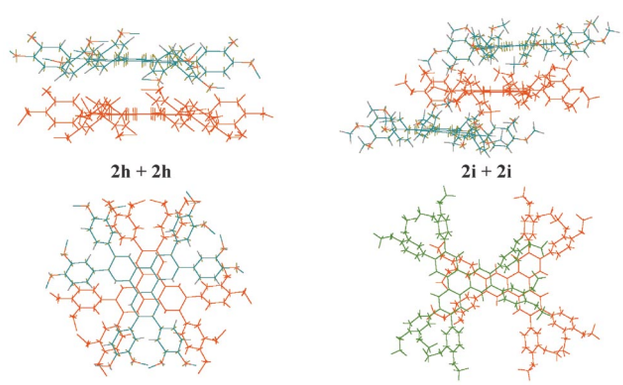

Fig. 5 Predicted minimum energy geometries of π-stacked dimers: left, PDQ201 (**2h**) homo-dimer (only one dock shown for clarity); right, PTP2O1 (**2i**) hetero-dimer. Upper figures show the side view and the lower show the plan view. The central (red) molecule is held fixed; the other molecules are the bullets that dock to the lowest energies.

homo-dimer containing PDQ1 (**2e**) (Fig. 5, left). The CPI now has a much bigger coulombic contribution from the interacting, peripheral phenyl groups. This results in a much more stable homo-dimer. The homo-dimer of PTP2O1 (**2i**) is, like that of PDQ2O1 (**2h**), predicted to be more stable than the HAT1 (**1b**) containing hetero-dimer. In this case the contributions to the destabilisation of ΔE were shown to originate primarily from the VDW term. In the PTP2O1 (**2i**) homo-dimer, the neighbouring molecules have their triphenylene cores slightly displaced, increasing the contact between the side-chains of one molecule and the peripheral phenyl groups of the other (Fig. 5, right). The coulombic interaction between the phenyl groups is apparently less important in this case.

The variable effects (either stabilising or otherwise) that are imposed by the peripheral phenyl groups are removed in xPTP2O1 (**4b**). The large planar aromatic cores now pack very well together and as a result the VDW contribution is the most dominant. The coulombic contribution to ΔE is also repulsive, a result that is consistent with the fact that xPTP2O1 (**4b**) and HAT1 (**1b**) have net quadrupoles with the same sign.

XED modelling of the CPI discotic liquid crystals (1–2): variations in the structure of the small core component

The effect of adding an α-substituent to HAT6 (in the form of nitro (**1c**) or two fluorine groups (**1e**)) upon the 1 : 1 ratio of compounds formed by mixing with PDQ9 (**2a**) and PTP9 (**2b**) is discussed in ref. 3. It was shown that with a small a substituent such as F, the CPI compound was able to form. The more bulky nitro group, however, disturbs the packing. NO_2-HAT6 (**1c**) forms a compound with PDQ9 (**2a**) that melts at a lower temperature than NO_2-HAT6 (**1c**). NO_2-HAT6 (**1c**) phase separates from PTP9 (**2b**), forming no stable compound.

The XED results correctly predict that the hetero-dimers are more stable than the homo-dimers (negative ΔE) for mixtures containing 2F-HAT1 (**1f**). For NO_2-HAT1 (**1d**) a stable mixture is predicted to form with PDQ1 (**2e**) but not with PTP1 (**2f**), perhaps explaining the different miscibilities observed (Table 8). Closer examination of the geometries and energies of the 250 docked dimers shows the NO_2-HAT1 (**1d**)–PDQ1 (**2e**) hetero-dimer has a far higher number of non-planar (liquid-like) docks at energies close to the global minimum than the HAT1 (**1b**)–PDQ1 (**2e**) hetero-dimer suggesting supporting the observed lowering of the melting point.

Table 8 Summary of the contribution to ΔE for NO_2-HAT1 (**1d**) and 2F-HAT1 (**1f**) hetero-dimers with PDQ1 (**2e**) and PTP1 (**2f**)

Molecule	ΔE_{VDW}/kcal mol^{-1}	ΔE_{coul}/kcal mol^{-1}	ΔE_{Total}/kcal mol^{-1}
NO_2-HAT1–PDQ1	−2.5	−0.6	−3.1
NO_2-HAT1–PTP1	−1.4	3.0	1.6
2F-HAT1–PDQ1	−4.2	−2.9	−7.1
2F-HAT1–PTP1	−1.1	−5.3	−6.4

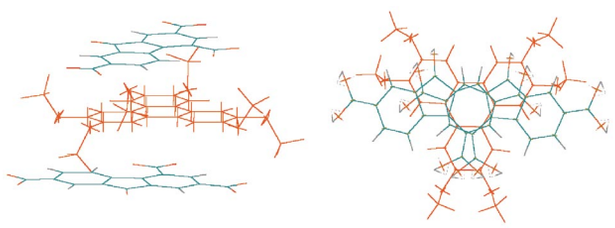

Fig. 6 Minimum energy geometry for the HAT1 (**1b**)–TNF (**3**) hetero-dimer. Left shows the perspective view and right shows the top view.

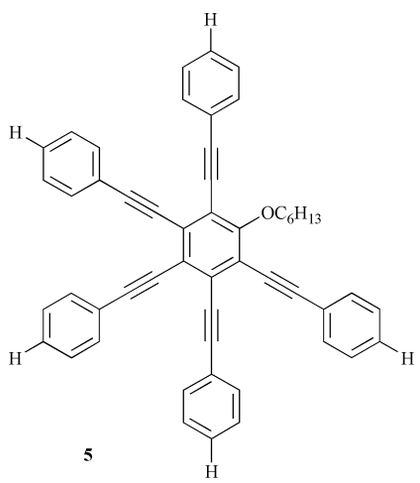

Fig. 7 Benzene multiyne **5**, analogues of which are known to form induced mesophases with TNF (**3**).[8]

XED modelling of HAT1 (1b) and TNF (3)

The 1 : 1 mixture of HAT1 (**1b**) and TNF (**3**) is predicted to be more stable than the components, as expected on the basis of experimental findings and previous theoretical models. The contributions to the stabilisation energy ΔE are 42% VDW and 58% electrostatic. The same has also been shown to be true for the alkoxy-triphenylenes HAT*n* (**1*n***), for n = 1–6.

The TNF (**3**) molecules in the homo-dimer are predicted to lie with the aromatic cores in parallel. The molecules are arranged such that the sides bearing two nitro groups are furthest from each other. In the HAT1 (**1b**)–TNF (**3**) hetero-dimer (shown in Fig. 6) the TNF molecules are arranged in such a way as to place two nitro groups and the carbonyl group over the triphenylene nucleus. The strong interaction between HAT*n* (**1*n***) and TNF (**3**) observed experimentally can therefore be successfully predicted using the XED force field.

XED modelling of benzene multiyne (5) and TNF (3)

The benzene multiyne (**5**, Fig. 7) also forms stable compounds with TNF (**3**); the origin of this stability has previously been attributed to charge-transfer or net quadrupolar interactions. The results of the XED experiments performed on **5** and **3** successfully reproduce the results of the net quadrupolar model, predicting that the hetero-dimer is the most stable. The results of the docking experiments are shown in Table 9.

The molecules in the homo-dimer of **5** are positioned such that the long alkyl chains are alternately on opposite sides of the aromatic core (Fig. 8). The minimum energy geometry of the **5**–TNF (**3**) hetero-dimer has the TNF nitro groups as near

Table 9 Summary of the XED docking experiments for multiyne (**5**) and TNF (**3**) homo-dimers and their hetero-dimers. All energies are quoted in kcal mol^{-1}

Molecule	E_{VDW}	E_{coul}	E_{Total}	ΔE
5–**5**	−43.21	−1.29	−44.50	
TNF (**3**)–TNF (**3**)	−16.43	−1.83	−18.26	
5–TNF (**3**)	−30.33	−4.82	−35.15	−3.7

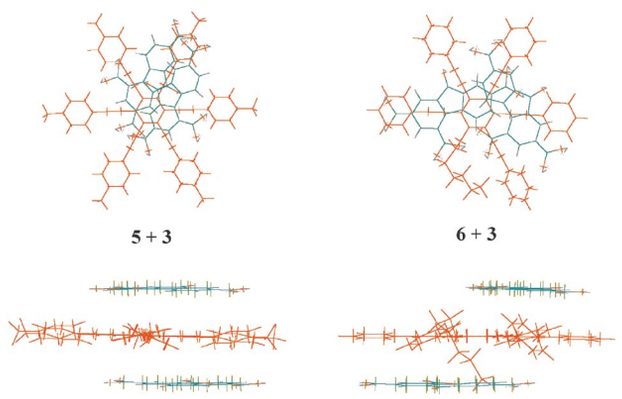

Fig. 8 Minimum energy geometries for the multiyne–TNF dimers. Right shows **5**–**5**, left shows **5**–TNF (**3**).

to the π-electrons of the neighbouring molecule as possible. The prediction of a stable mixture in each case suggests that charge-transfer alone cannot be responsible for the π–π interactions, which contribute to the observed stability of the mixtures.

XED modelling of arene–perfluoroarene interactions[9]

Dai *et al.* recently published a study of the phases formed by mixtures of 1,4-bis(4-phenylethynyl)benzenes (BPEB **6**–**9**, Scheme 2) bearing complementary patterns of fluorine substitution.[9] They showed that the arene–fluoroarene interaction favoured formation of 1 : 1 mixtures in a similar way to the CPI

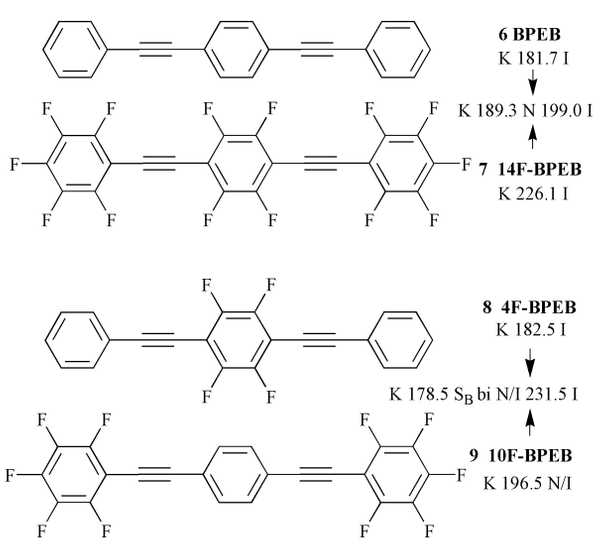

Scheme 2 Selectively fluorinated 1,4-bis(4-phenylethynyl)benzenes (*n*F-BPEB) **6**–**9**.[9]

Table 10 Energies for the minimum energy conformations of molecular dimers of fluorinated BPEBs (**6**–**9**) and their complementary mixtures as predicted by the docking routine

Molecule	E_{VDW}/kcal mol^{-1}	E_{coul}/kcal mol^{-1}	E_{Total}/kcal mol^{-1}	ΔE_{VDW}/kcal mol^{-1}
6	−16.11	−3.93	−20.03	
7	−25.14	−3.12	−28.27	
8	−22.47	−1.36	−23.84	
9	−23.46	0.72	−22.74	
6–**7**	−26.64	−4.42	−31.06	−6.0
8–**9**	−23.93	−3.37	−27.3	−0.8

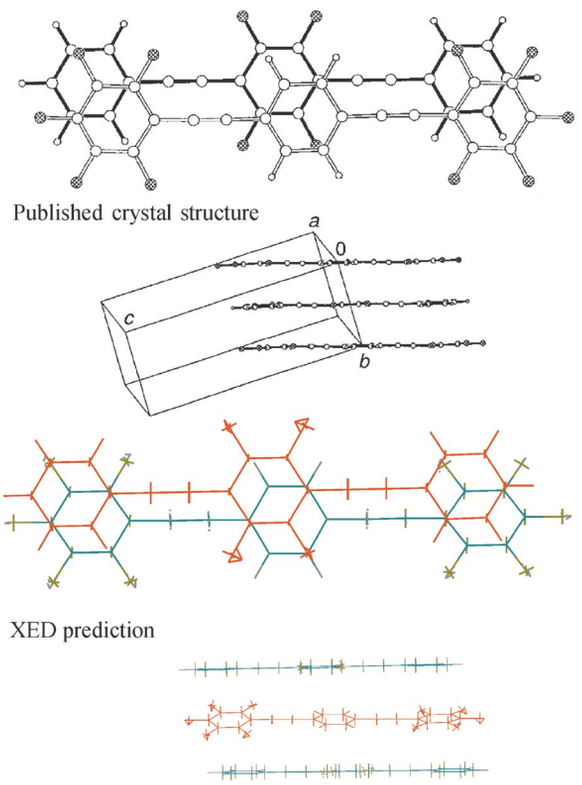

Fig. 9 Comparison of published X-ray crystal structures and XED predictions for the dimer of 14F-BPEB (**9**, red) and 4F-BPEB (**8**, blue): upper, X-ray crystal structure (adapted from ref. 9); lower, minimum energy conformation produced by the XED docking procedure.

compounds. As was the case with our mixtures, the researchers observed no evidence of charge-transfer interactions.

The 1 : 1 mixture of the non-mesogens BPEB (**6**) and 14F-BPEB (**7**) produces a compound with a lower melting point than one of the components, but a nematic liquid crystal phase is induced. The 1 : 1 molar mixture of 4F-BPEB (**8**) and 10F-BPEB (**9**) has a higher clearing point than either of the components and exhibits an induced smectic (S_B) phase. The results of docking for the homo- and complementary hetero-dimers are shown in Table 10. Fig. 9 shows a comparison between the X-ray crystal structure of **8** and **9** and the minimum energy conformation predicted by the XED force field. The two are again in good agreement.

Conclusion

Our particular interest in π-stacked systems arose from the need to design discotic liquid crystals with enhanced one-dimensional conductivity and mesophase ranges[4] but this problem is of fundamental significance in materials science, biochemistry, molecular engineering, nano-technology, *etc*. In some cases the observation of charge-transfer bands in alternating two component "stacks" leads to the suggestion that this was an important binding interaction. In other cases net quadrupolar interactions, dispersed multipole interactions and steric interaction have been involved. However, perhaps the most generally applicable treatment is the XED method[7] and in this paper we have extended this method to model π-stacked systems including HAT–TNF, benzene–hexafluorobenzene, triphenylene–perfluorotriphenylene, benzene multiyne–TNF and complementary mixtures of selectively fluorinated 1,4-bis(phenylethynyl)benzenes. This will prove an invaluable tool in developing π-stacking "synthons" in supramolecular chemistry as an alternative to the more frequently exploited hydrogen bond.

References

1 M. Finkelstein, S. A. Hart, W. M. Moore, S. D. Ross and L. Eberson, *J. Org. Chem.*, 1986, **51**, 3548; L. Eberson and S. S. Shaik, *J. Am. Chem. Soc.*, 1990, **112**, 4484; P. Carloni, L. Greci, P. Stipa and L. Eberson, *J. Org. Chem.*, 1991, **56**, 4733; L. Eberson, *New J. Chem.*, 1992, **16**, 151; L. Eberson, B. Olofsson and J. O. Svensson, *Acta Chem. Scand.*, 1992, **46**, 1005; L. Eberson, O. Persson and F. Radner, *Res. Chem. Intermed.*, 1996, **22**, 799; N. Johansson, T. Kugler, L. Eberson and W. R. Salaneck, *Acta Chem. Scand.*, 1998, **52**, 275.

2 E. O. Arikainen, N. Boden, R. J. Bushby, O. R. Lozman, J. G. Vinter and A. Wood, *Angew. Chem., Int. Ed.*, 2000, **39**, 2333.

3 N. Boden, R. J. Bushby, G. Cooke, O. R. Lozman and Z. Lu, *J. Am. Chem. Soc.*, 2001, **123**, 7915.

4 N. Boden, R. J. Bushby, G. Headdock, O. R. Lozman and A. Wood, *Liq. Cryst.*, 2001, **28**, 139; T. Kreouzis, K. Scott, K. J. Donovan, N. Boden, R. J. Bushby, O. R. Lozman and Q. Liu, *Chem. Phys.*, 2000, **262**, 489; T. Kreouzis, K. J. Donovan, N. Boden, R. J. Bushby, O. R. Lozman and Q. Liu, *J. Chem. Phys.*, 2001, **114**, 1797.

5 M. A. Bates and G. R. Luckhurst, *Liq. Cryst.*, 1998, **24**, 229.

6 A. Hunter and J. K. M. Sanders, *J. Am. Chem. Soc.*, 1990, **112**, 5525.

7 J. G. Vinter, A. Davis and M. R. Saunders, *J. Comput.-Aided Mol. Des.*, 1987, **1**, 31; J. G. Vinter, *J. Comput.-Aided Mol. Des.*, 1994, **8**, 653; J. G. Vinter, *J. Comput.-Aided Mol. Des.*, 1996, **10**, 417.

8 K. Praefcke, D. Singer and A. Eckert, *Liq. Cryst.*, 1994, **16** , 53; K. Praefcke, D. Singer, B. Kohne, M. Ebert, A. Liebmann and J. H. Wendorff, *Liq. Cryst.*, 1991, **10**, 147.

9 C. Dai, P. Hguyen, T. B. Marder, A. J. Scott, W. Clegg and C. Viney, *Chem. Commun.*, 1999, **24**, 2493.

10 MOPAC and SIMPLEX as implemented in the XED modelling suite, J. G. Vinter, Cambridge, 1996.

11 N. L. Allinger, *Calculation of Molecular Structure and Energy by Force-field methods*, in *Advances in Physical Organic Chemistry*, ed. V. I. Gold and D. Bethell, Academic Press, Cambridge, 1976.

12 T. Dahl, *Acta Chem. Scand.*, 1973, **27**, 995; D. A. Doherty and J. C. Ma, *Chem. Rev.*, 1997, **97**, 1303.

13 M. Weck, A. R. Dunn, K. Matsumoto, G. W. Coates, E. B. Lobkovsky and R. H. Grubbs, *Angew. Chem., Int. Ed.*, 1999, **38**, 2741.

14 R. J. Bushby and G. J. Ferber, *J. Chem. Soc., Perkin Trans. 2*, 1976, 1695; R. J. Bushby and H. L. Steel, *J. Chem. Soc., Perkin Trans. 2*, 1990, 1169; R. J. Bushby, H. L. Steel and M. P. Tytko, *J. Chem. Soc., Perkin Trans. 2*, 1990, 1155; R. J. Bushby and H. L. Steel, *J. Chem. Soc., Perkin Trans. 2*, 1990, 1143.

15 S. L. Price and A. J. Stone, *J. Chem. Phys.*, 1987, **86**, 2859.

16 A. P. West, S. Mecozzi and D. A. Dougherty, *J. Phys. Org. Chem.*, 1997, **10**, 347.

17 J. H. Williams, *Acc. Chem. Res.*, 1993, **26**, 593.

18 N. Boden, R. J. Bushby, M. V. Jesudason and B. Sheldrick, *J. Chem. Soc., Chem. Commun.*, 1988, 1342.

19 T. Wang, D. Yan, J. Luo, E. Zhou, O. Karthaus and H. Ringsdorf, *Liq. Cryst.*, 1997, **23**, 869.